Oceanic pathways of an active Pacific Meridional Overturning Circulation (PMOC)

Matthew D. Thomas, Alexey V. Fedorov, Natalie J. Burls, Wei Liu

Geophysical Research Letters

RESEARCH LETTER
10.1029/2020GL091935

Oceanic Pathways of an Active Pacific Meridional Overturning Circulation (PMOC)

M. D. Thomas[1,2], **A. V. Fedorov**[1,3], **N. J. Burls**[4], **and W. Liu**[5]

[1]Department of Earth and Planetary Sciences, Yale University, New Haven, CT, USA, [2]Now at University Corporation for Atmospheric Research, Boulder, CO, USA, [3]LOCEAN-IPSL, Sorbonne University, Paris, France, [4]Department of Atmospheric, Oceanic, & Earth Sciences, George Mason University, Fairfax, VA, USA, [5]Department of Earth and Planetary Sciences, University of California, Riverside, CA, USA

Abstract In contrast to the modern-day climate, North Pacific deep water formation and a Pacific meridional overturning circulation (PMOC) may have been active during past climate conditions, in particular during the Pliocene epoch (some 3–5 million years ago). Here, we use a climate model simulation with a robust PMOC cell to investigate the pathways of the North Pacific deep water from subduction to upwelling, as revealed by Lagrangian particle trajectories. We find that similar to the present-day Atlantic Meridional Overturning Circulation (AMOC), most subducted North Pacific deep water upwells in the Southern Ocean. However, roughly 15% upwells in the tropical Indo-Pacific Oceans instead—a key feature distinguishing the PMOC from the AMOC. The connection to the Indian Ocean is relatively fast, at about 250 years. The connection to the tropical Pacific is slower (~800 years) as water first travels to the subtropical South Pacific then gradually upwells through the thermocline.

Plain Language Summary Deep water formation may have occurred in the North Pacific Ocean during the Pliocene, enabling a Pacific Meridional Overturning Circulation (PMOC) that is absent in today's ocean. Here we trace water particles in a Pliocene-like climate model, in which a PMOC has developed, to determine the subsurface pathways and destinations of the PMOC water after sinking from its surface source regions. As with the present-day Atlantic overturning, most water upwells in the Southern Ocean. However, roughly 15% of the PMOC water returns to the surface in the tropical Pacific and Indian oceans. Such pathways are weak in the Atlantic overturning system and represent a unique feature of the PMOC and its contribution to the ocean environment of the Pliocene and possibly other past climate states.

Key Points:

- Lagrangian particles are used to assess the global pathways and timescales of the Pacific meridional overturning circulation (PMOC)
- After subduction most of the PMOC water returns to the surface in the Southern Ocean on centennial to millennial timescales, similar to the Atlantic meridional overturning circulation
- Approximately 15% of the PMOC water upwells in the tropical Pacific and Indian oceans on centennial timescales—a feature unique to the PMOC

Supporting Information:

Supporting Information may be found in the online version of this article.

Correspondence to:

M. D. Thomas,
matthewt@ucar.edu

Citation:

Thomas, M. D., Fedorov, A. V., Burls, N. J., & Liu, W. (2021). Oceanic pathways of an active Pacific meridional overturning circulation (PMOC). *Geophysical Research Letters*, *48*, e2020GL091935. https://doi.org/10.1029/2020GL091935

Received 9 DEC 2020
Accepted 27 APR 2021
Corrected 2 JUN 2021

This article was corrected on 2 JUN 2021. See the end of the full text for details.

1. Introduction

An essential element of modern ocean circulation and climate is the Atlantic Meridional Overturning Circulation (AMOC), which through deep water formation in the subpolar North Atlantic, gives rise to the northward transport of heat, freshwater, and nutrients through the basin. While a comparable circulation is currently absent in the Pacific, the possibility of deep water formation in the North Pacific and an active meridional overturning circulation there has attracted growing attention recently, both in the paleo context (e.g., Burls et al., 2017; Liu & Hu, 2015) and in theoretical studies of ocean circulation (Ferreira et al., 2018; Jones & Cessi, 2016). The lack of Pacific deep water formation and meridional overturning in the modern climate has been primarily attributed to the presence of relatively fresh surface water in the subarctic Pacific (e.g., Warren, 1983) which inhibits deep mixing and downwelling. These fresh conditions are explained by the local excess of precipitation over evaporation in the northern Pacific due to net moisture transport from the Atlantic to the Pacific (Stocker & Wright, 1991) and/or moisture transport associated with the Asian monsoon (Emile-Geay et al., 2003). Some studies argue that the lack of deep water formation in the Pacific is a consequence of the occurrence of MOC in the Atlantic (Saenko et al., 2004), while others suggest that the smaller width of the Atlantic predisposes it to high salinity and deep water formation (Ferreira et al., 2010; Jones & Cessi, 2017); idealized coupled simulations with no orography tend to develop a PMOC (Schmittner et al., 2011).

The possibility of an active PMOC during the warm Pliocene epoch, having CO_2 atmospheric concentrations comparable to today's elevated levels, has drawn particular attention since the Pliocene may provide

an analog for future global warming. Available evidence for a Pliocene PMOC, including North Pacific records of calcium carbonate ($CaCO_3$) accumulation, biological productivity, $\delta^{13}C_{benthic}$ and redox-sensitive trace metals as well as modeling results, has been summarized in Burls et al. (2017).

How was this active PMOC maintained during the Pliocene? Pliocene reconstructions of deep ocean temperatures within the Pacific reflect 0°–3°C of warming (Lear et al., 2000; Woodard et al., 2014), while SST reconstructions from the North Pacific indicate between approximately 3°–6°C of warming (LaRiviere et al., 2012; Pagani et al., 2010). Therefore, as in the Atlantic, the Pliocene ocean temperature changes alone would have acted to stratify the North Pacific inhibiting deep water formation. However, climate modeling results suggest that the mean warmth and reduced meridional SST gradients of the Pliocene can support large-scale changes in the hydrological cycle (Burls & Fedorov, 2014, 2017; Burls et al., 2017), weakening the stratification in the North Pacific. In particular, the reduced tropical to subtropical SST gradient maintains a weaker atmospheric Hadley circulation and subtropical high-pressure systems, reducing moisture transport from the subtropics to the tropics and midlatitudes. Results from fully coupled simulations with the Community Earth System Model (CESM) indicate that these changes in the hydrological cycle can indeed weaken the salinity-controlled density stratification in the North Pacific to the point that deep water formation occurs, resulting in a PMOC and North Pacific deep water formation (Burls et al., 2017).

How the presence of an active PMOC contributes to the tracer distribution and biogeochemistry of the Pliocene depends on the inter-connectivity of the PMOC water with the rest of the global ocean. Using a present-day simulation with an active AMOC and a Pliocene-era simulation with both an active PMOC and an AMOC, in this study we build on the results of Burls et al. (2017) by isolating the surface origins and final destinations of the PMOC water, determining the pathways and transit timescales between them and identifying how these characteristics differ from that of the AMOC. A particular focus is on the North Pacific deep water that eventually upwells into the tropical Pacific, which is indicated by the model Indo-Pacific streamfunction to be a feature that is clearly distinct from the AMOC (Figures 1, S1 and S2, and Burls et al., 2017).

Due to difficulties in determining the pathways, endpoints and relative transports of the various different water masses using streamfunctions derived from a zonally averaged transport field (Haertel & Fedorov, 2012), here we use a Lagrangian ocean analysis to precisely target the waters that are ventilated into the permanent thermocline through mixed layer subduction in the northern North Pacific and subsequently trace their advective pathways through the rest of the global oceans. This provides a direct determination of the locations, pathways, and timescales of inter-connectivity of an active PMOC (see Methods). Our analysis goes beyond the Pliocene climate as it provides a general qualitative description of ocean water pathways in the presence of the Pacific deep water formation.

2. Methods

2.1. Numerical Model

We have applied our Lagrangian analysis (see description below) to the output from the CESM version 1.0.4. It is a fully coupled climate model (Danabasoglu et al., 2012) that has been further modified to simulate a Pliocene-like climate (Burls & Fedorov, 2014; Burls et al., 2017). The model base configuration employs an ocean and sea-ice horizontal resolution that increases from 1° near the equator to 3° near the poles, with a displaced-pole centered over Greenland to avoid polar singularity, and a vertical resolution of 50 layers that increase in thickness with depth (the gx3v7 grid). The atmospheric and land component horizontal resolutions are spectral, with a truncation cutoff at 31 levels (the T31 configuration) and 26 vertical levels. The ocean model has coefficients for horizontal and vertical tracer eddy diffusivity of $\kappa_h = 4 \times 10^3$ m^2 s^{-1} and $\kappa_v = 1.6 \times 10^{-5}$ m^2 s^{-1}, respectively. It also employs the Gent and McWilliams (Gent & McWilliams, 1990) parametrization for isopycnal eddy tracer mixing and the corresponding eddy-induced velocity (EIV) using a coefficient of $\kappa_{GM} = 4 \times 10^3$ m^2 s^{-1}, and K-profile parametrization for diapycnal mixing (Large et al., 1994; see Figure S13 in Burls et al., 2017 for mixing rates). A control simulation using preindustrial levels of atmospheric CO_2 has been spun up for 3,000 years.

The model Pliocene-like conditions, which were characterized in the ocean by the reduced meridional temperature gradients between the equator and the extra-tropics, were simulated by modifying the cloud reflectivity of the model atmosphere (Burls et al., 2017). This has been achieved by modifying the atmosphere

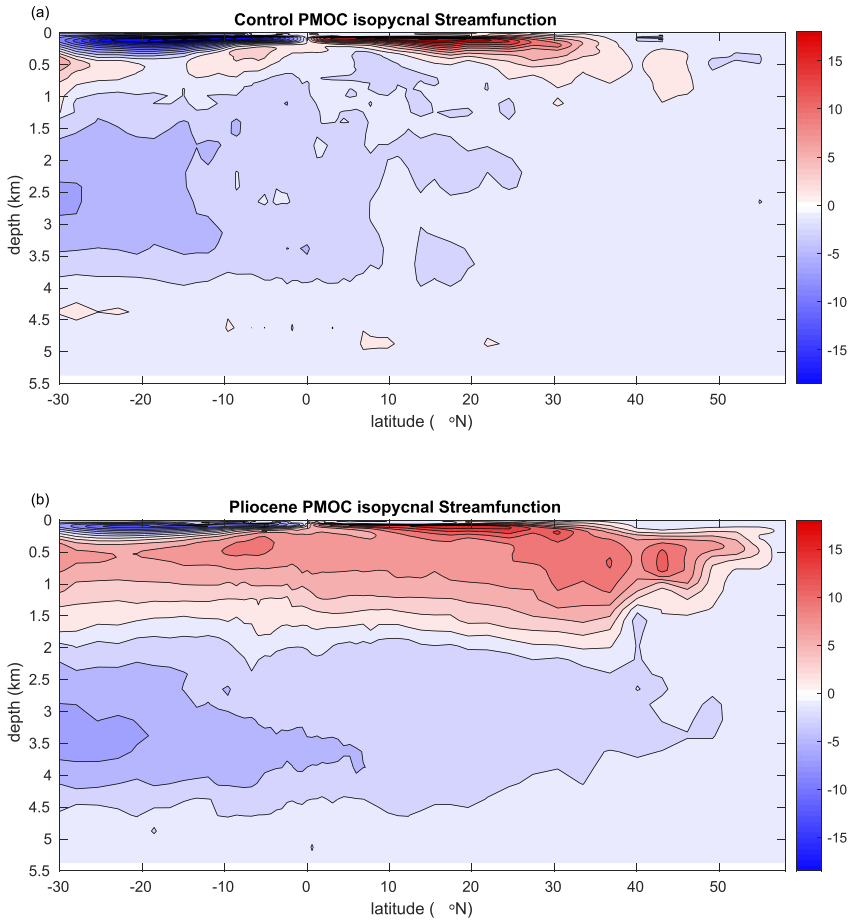

Figure 1. Meridional overturning streamfunction for the Indo-Pacific oceans in (a) the Control and (b) Pliocene experiments. The streamfunction is calculated in density coordinates and re-mapped back onto the depth coordinates using the mean depth of the time-dependent density fields. Units are Sv (10^6 m^3 s^{-1}), and contour intervals are 2 Sv.

liquid water path everywhere poleward of 15° latitude, and the ice and water paths everywhere equatorward of 15° latitude in the shortwave radiation scheme such that the tropical albedo was increased by 0.06 and the extratropical albedo was reduced by 0.04. This produces a simulation of the Pliocene that is more realistic (relative to proxy-observational data) than the modeling efforts that have employed increased atmospheric CO_2 concentrations, which have typically required unrealistically high concentrations (and correspondingly high global temperatures; Fedorov et al., 2015). The water path modifications were applied to a simulation with the same boundary conditions and initialized from the same initial conditions as the preindustrial control simulation and subsequently run for 4,000 years over which the model PMOC developed. An approximate steady state was reached after 1,500 years (see Burls et al., 2017, Figure S4, for time series of the overturning spin-up phase). The Pliocene experiment is longer to ensure that it has reached equilibrium (as the PMOC is activated only by the end of the first 1,000 years of the run).

Time-averaged streamfunctions of the Pliocene PMOC (Figure 1) and AMOC (Figure S1) have maxima at 11.7 and 7.9 Sv, respectively, when calculated in density coordinates, as compared to the AMOC control maximum of 15.4 Sv. These numbers are for the last 100 years of each experiment. We note that in depth space the subtropical overturning values (~17 Sv for the Pliocene PMOC as reported in Burls et al., 2017, and shown in Figure S2) are larger than the density space ones used here due to the presence of a depth-space subtropical overturning cell that arises from the western upwelling and eastern downwelling (e.g., Spall, 1992), and which is often weaker in density space in models (see e.g., the stronger depth-space subtropical AMOC strength in figures in the work of Johnson et al., 2019; Ortega et al., 2017). A full description

of the model setup can be found in the work of Burls and Fedorov (2014) and Burls et al. (2017) along with details of the simulation's agreement with paleo-proxy observational data.

2.2. Lagrangian Analysis

The Lagrangian ocean analyses have been performed for this study using the Ariane software package (Blanke & Raynaud, 1997, http://www.univ-brest.fr/lpo/ariane). Ariane calculates an analytical solution of model particle trajectories according to the output velocity fields of an ocean model. Particles can be seeded at any location or time in the model (including at higher resolution than the model grid), and their trajectories can be calculated forward or backward in time so as to determine the water-mass destinations or origins, respectively. Particle trajectory information of position, properties and volume transport (Blanke & Raynaud, 1997) can be provided at every timestep or, to reduce disk storage requirements, just the end-point locations can be saved. By using the velocity calculations from the model momentum equations and from the model EIVs, the particle trajectories represent the advective pathways of water parcels in isolation of the effects of parametrized tracer diffusion (We note that the model also includes a submesoscale velocity parametrization in the mixed layer, which is not relevant in this study in which particles are constrained below the mixed layer). We apply the Ariane package to 100 years of both the Control and Pliocene simulations during which the overturning circulations were stable, years 3,000–3,100 and years 4,000–4,100, respectively (the final 100 years of the simulations). This time period allows for long Lagrangian experiments while also avoiding any significant centennial-scale changes or property trends (as well as storage limitations). Since the global overturning circulation requires many thousands of years for ventilated water to return to the ocean surface, the long timescales have been resolved by looping particle trajectories over the model 100 years of data (van Sebille et al., 2018). To determine the sensitivity to looping over a discontinuity, a repeat experiment was run with two additional temporal discontinuities introduced by reordering years 67–100 before 34–66. These additional discontinuities led only to small-scale regional differences with the results shown in Figure 2 and affected none of the large-scale patterns or values.

The experimental setup is designed to first identify the mixed layer source regions of deep water and subsequently, determine the mixed layer destinations of the water ventilated from those sources. Particles are seeded in every grid cell of each ocean basin along 25°N and at every timestep of the 100-year period. Particles are integrated first backward in time, toward the mixed layer source regions at high northern latitudes, and then stopped upon reaching the model mixed layer (defined according to a density difference of 0.01 kg m^{-3} between the ocean surface and the base of the mixed layer; Thomas & Fedorov, 2017). Figure S3 shows the average particle transport of mixed layer subduction for all backward trajectories that subducted from the mixed layer of the North Pacific domain, calculated in Sv (10^6 m^3 s^{-1}). All particles originating close to the northern basin margin (north of ~40°N) are then identified (Figure 2a) and run forward in time from their 25°N starting positions. They are run in a global domain and stopped when they once again return to the mixed layer (Figure 2b). These computations were applied separately for particles in the Pacific and Atlantic (Figure S4) oceans of the Pliocene run and to particles in the Atlantic Ocean of the Control run (Figure S5). A starting latitude of 25°N was chosen as one that is close to the deep water source regions while still capturing the separation of subpolar and subtropical subduction; however, the Lagrangian identification of the source regions is not sensitive to this choice. Positional information of the (~1 million) particles in each experiment is only saved at the end-point positions, at the particle mixed layer origins and destinations. Along-path trajectories are then saved to highlight the particle pathways for various subsets of the particle destinations in each experiment, selecting sets of 12,000 particles in each case.

In the forward experiments, some particles inevitably remain in the ocean subsurface even after thousands of years of integration time. These are considered lost to the calculation. However, over 90% of the particles have been accounted for in all the experiments, and we assume that the uncounted particles are unlikely to represent any single pathway through the deep ocean when considered on such a long timescale. All particle percentages reported below are therefore made relative to the particle transport that was captured in our experiments.

Ariane is a powerful tool with a specific capability to track millions of particles while avoiding computing and file storage issues by saving only the particle end-point positions. It was, however, originally designed to work with ocean models configured on an Arakawa C-grid (Arakawa & Lamb, 1977), yet the CESM ocean

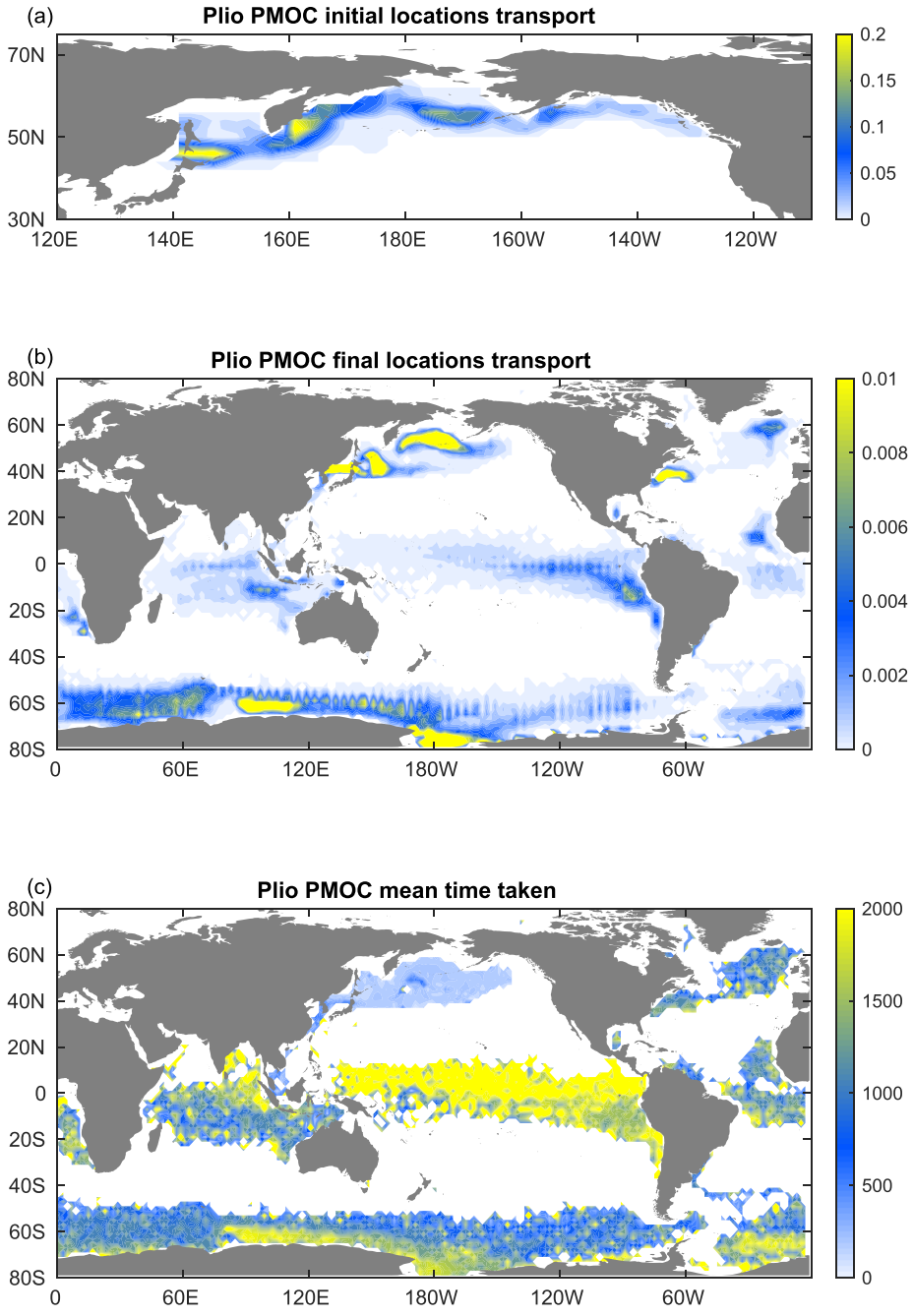

Figure 2. Mean particle transport (in Sv) at the mixed layer (a) origins and (b) destinations of the PMOC water within the model Pliocene run, determined according to forward-trajectories and back-trajectories of model Lagrangian particles (see methods for the experimental design). Particle transports have been binned onto a 2° × 2° grid and averaged. (c) Mean travel time for all particles ending within each grid cell (in years).

component is configured on an Arakawa B-grid. The B-grid velocities are therefore first linearly interpolated onto a C-grid configuration in a manner that preserves mass continuity. To overcome technical problems encountered because of large EIV values located mostly at the ocean boundaries of the model that cause the program to crash, possibly due to nondifferentiable trajectory solutions or an unrealistic propagation of particles, the EIVs were set to zero at the ocean boundaries as well as in those places where EIVs exceed the 99th percentile of all EIV velocities. The removal method preserves mass continuity. Test experiments using a Pacific-only domain (where the boundary EIV problem is much reduced) demonstrate that the particle

trajectories are weakly sensitive to this EIV removal and that our conclusions are unaffected by it. To the authors' knowledge, this manuscript documents the first successful use of Ariane for tracing particles in the output of a B-grid model.

3. Results

The Lagrangian particles pinpoint the North Pacific mixed layer regions of the Pliocene simulation that source water to the lower limb of the PMOC (Figure 2a). These regions are located close to the northern margin of the Pacific basin, primarily in three hotspots of similar strength in the Bering Sea and off the coast of Kamchatka where surface densities become high enough to mix with the deep ocean (Burls et al., 2017). As with the AMOC (Figure S4a), subduction occurs close to the topographic boundary of the subpolar gyre (e.g., Thomas et al., 2015) where dynamical constraints on subduction into the permanent thermocline are satisfied (Spall & Pickart, 2001). The regions are distinct from, and further to the north of, those regions that source water to the shallow subtropical cells (McCreary & Lu, 1994; Thomas & Fedorov, 2017). The net particle transport of the PMOC water is 9.1 Sv, a value that represents the overturning that can be traced throughout the basin back to the northernmost source regions, that is, the meridionally coherent component of the PMOC in the absence of local overturning circulation cells. For the Atlantic particles, the net transports are 11.3 and 6.2 Sv for the Control and Pliocene runs, respectively.

Upon tracing those particles through the lower limb of the overturning cell, the final obducted locations of the particles demonstrate the global reach of the PMOC water (Figure 2b), with most water returning to the mixed layer in the Southern Ocean (~57% of the isolated PMOC water) after traveling the full latitudinal extent of the Pacific primarily along the western boundary of the basin. While the PMOC water is returned to the mixed layer at locations throughout the Southern Ocean, there are regional hotspots of obduction located principally within the Ross Sea and within the Indian Ocean sector of the Southern Ocean. Qualitatively, the findings are similar to those of the modern-day AMOC (Döös & Coward, 1997; Haertel & Fedorov, 2012; Toggweiler & Samuels, 1995) for which most North Atlantic Deep Water originating from the surface of the high latitude North Atlantic is eventually upwelled back into the surface mixed layer of the Southern Ocean through wind-induced surface Ekman divergence (Kuhlbrodt et al., 2007). A repeat experiment for Lagrangian particles seeded into the AMOC water of the Pliocene run (Figure S3) reveals that the North Atlantic water upwells within similar obduction sites in the Southern Ocean but with a larger proportion of ~77% of the water returning to the surface here (as explained below).

While the Control AMOC water also predominantly upwells within the Southern Ocean (some 71% of the water), important differences to the Pliocene AMOC are that the Control AMOC water obducts into different sites that are primarily located within the Atlantic and Indian Ocean sectors of the Southern Ocean and also located further to the north of the Antarctic coastline (Figure S5). This meridional offset is due to a southward shift of the Southern Ocean winds in the Pliocene run, and accordingly also of the Deacon Cell, which upwells deep water from further south (Figures S6 and S7). With the addition of reduced sea ice in the warmer Pliocene climate (Figure S8), relatively more water can accordingly obduct into regions such as the Ross Sea where the ice shelf of the modern climate otherwise acts as more of a barrier to wind-driven mixing and upwelling. The lower percentage of the Control AMOC water entering the Southern Ocean, relative to the Pliocene, is mostly offset by a larger percentage of water recirculating and upwelling in the subpolar North Atlantic, 23% versus 17%, respectively.

Pathways and timescales of transit toward the Southern Ocean are qualitatively similar for both the PMOC (Figure 3) and the AMOC (for both the Pliocene and Control simulations; Figure S6 and Figure S7, respectively), with water particles transported southward along western boundaries throughout the full meridional extent of each basin. Upon reaching the Southern Ocean, the water is then zonally transported around the Antarctic Circumpolar Current (ACC) before (after multiple laps; van Sebille et al., 2013) reaching their eventual respective mixed layer obduction regions. Particles are efficiently entrained into the ACC, possibly due to high model mixing rates in this region. The mean travel times for PMOC water to reach its major sites of mixed layer obduction back into the surface of the Southern Ocean vary from about 750 years for regions between 10° and 80°E, and about 1,000–1,500 years for regions located everywhere else (Figure 2). This is longer than the time for the AMOC water to reach those same destinations in the Pliocene (Figure S4). The

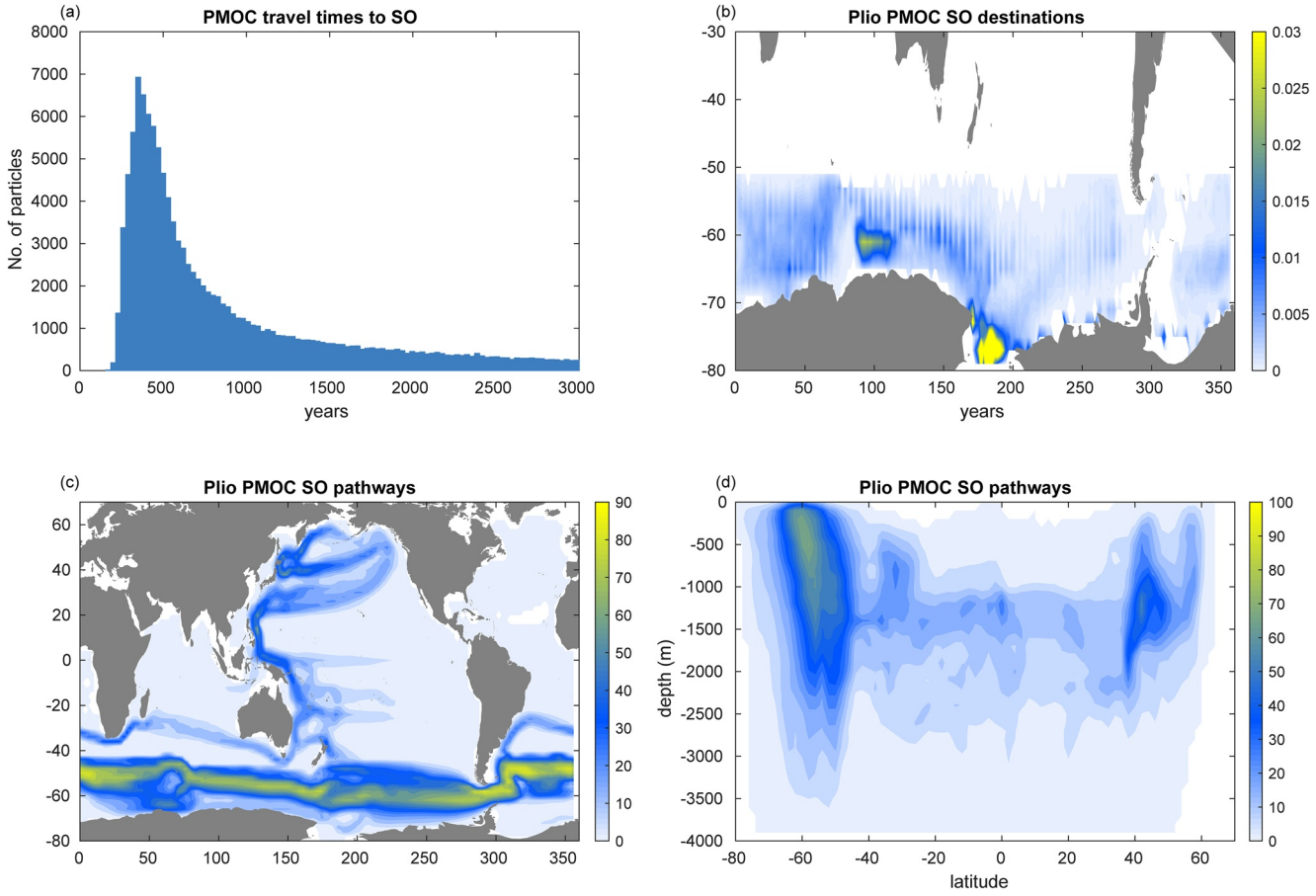

Figure 3. For all Pliocene PMOC water sinking in the subarctic North Pacific and upwelling in sites south of 50°S in the Southern Ocean: (a) Histogram of the travel times, (b) mean particle transports at the final upwelling destinations (in Sv, calculated as described in Figure 2), (c) the longitude-latitude pathways, and (d) the latitude-depth pathways. Pathways in (c) ans (d) use the along-track information (see Section 2.2) and are calculated as the percentage number of all unique particles that cross each grid cell of the 2° × 2° horizontal plane (at any depth) or the 2° × 100 m vertical cross section (at any longitude), at least once, for this subset of particles (which in effect shows the density of parcel trajectories). PMOC, Pacific meridional overturning circulation.

reasons for the faster AMOC travel times are not fully clear, although it could be related to the more southward extent of the Atlantic western boundary providing a direct route to the ACC (Figures S6 and S7). We note that when interpreting the maps of average age, the averages are strongly skewed by the long-tailed age distributions (Figures 3a and S6a–S7a).

One of the major differences between the Pliocene PMOC and the (Pliocene and Control) AMOC is a relatively high percentage of ~15% of PMOC water that upwells in the tropical band of the Pacific and Indian oceans (Figures 2, S4 and S5; Burls et al., 2017; Kuhlbrodt et al., 2007) along with ~2% in the tropical Atlantic. These upwelling regions correspond closely to regions of wind driven upwelling (Xie & Hsieh, 1995). This can be compared to the Control AMOC water for which ~1.9% upwells in the Indo-Pacific and ~3.4% in the tropical Atlantic and the Pliocene AMOC, with ~2.4% and ~1.3%, respectively. The Atlantic tropical upwelling is dominated by a region close to the Benguela upwelling zone (about 1.4% of the total Control AMOC water) which is on the fringe of the tropical Atlantic. The PMOC tropical connectivity is consistent with the relatively large tropical upwelling that occurs in the Pacific, combined with reduced stratification of the upper 100–300 m of the tropical band of the Pliocene simulation relative to the Control (Burls et al., 2017). Such a tropical advective connection to a high latitude water source raises the possibility, for example, of modified nutrient pool concentrations, CO_2 outgassing, or cold tongue temperatures in the tropical Pliocene ocean, but this will depend strongly on the timescales and exact pathways of such a connection (e.g., Thomas & Fedorov, 2017).

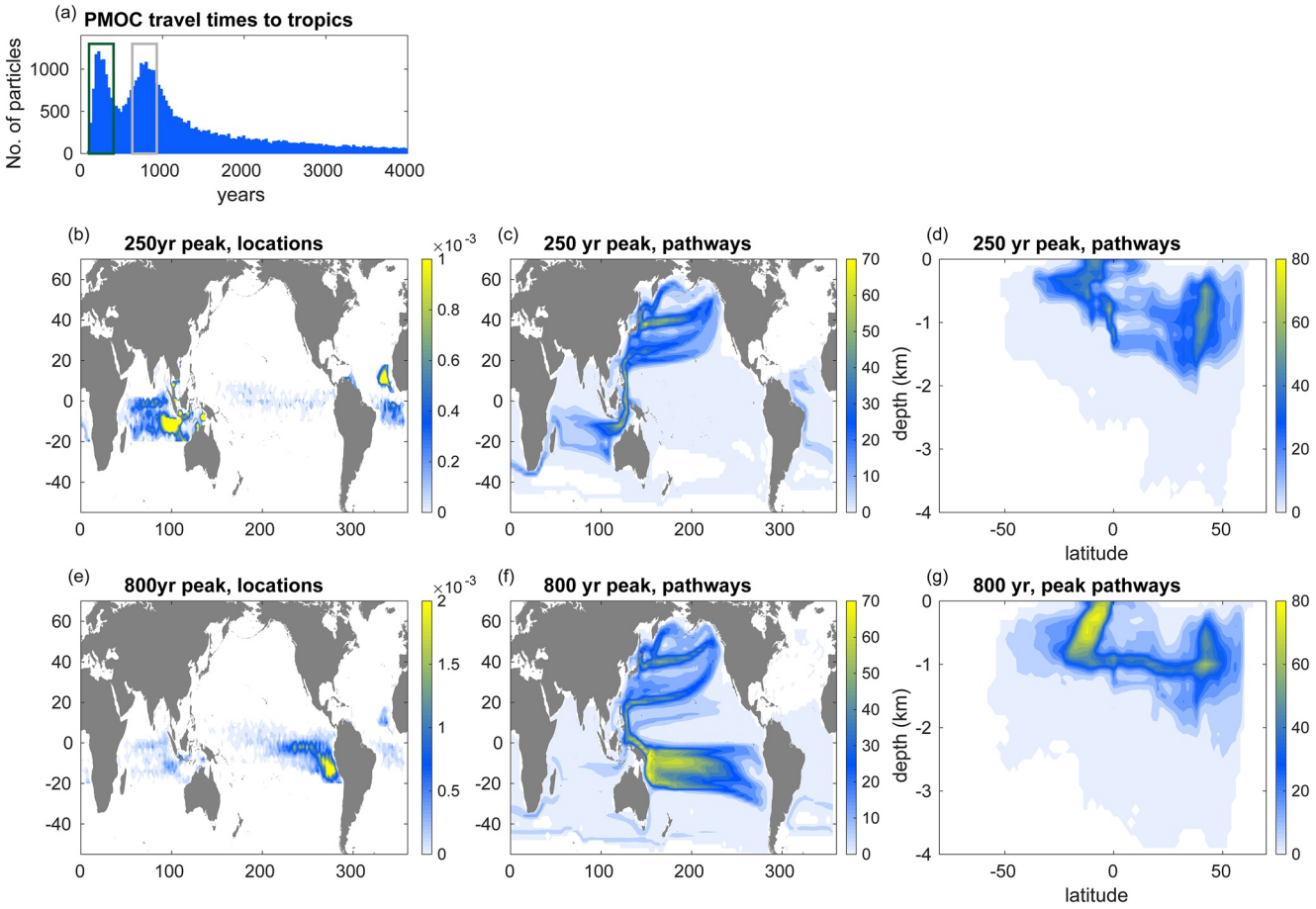

Figure 4. (a) Histogram of the travel times between the PMOC source regions and upwelling locations in the tropical ocean between latitudes 20°S and 20°N. The (b) and (e) mean particle transports at the final upwelling destinations (in Sv, calculated as described in Figure 2), (c) and (f) latitude-longitude pathways and (d) and (g) latitude-depth pathways of particles associated with the (b)–(d) shorter (green box) and (e)–(g) longer (gray box) dominant travel time peaks identified in (a) for water traveling between the PMOC source regions and the tropical band (see methods section). The pathways are calculated as in Figure 3. PMOC, Pacific meridional overturning circulation.

While average travel times for the PMOC water to obduct into the tropical band are longer than 1,000 years in many areas, travel timescales toward those geographical regions with the highest obduction rates are typically less than 1,000 years (Figures 2b and 2c). The distribution of travel times of those particles that obduct into the tropics reveals two distinct peaks centered at approximately 250 and 800 years (Figure 4a). Isolating the destinations and pathways of all the particles with tropical travel times falling within a 300-year window centered on each of these two peaks (Gray boxes in Figure 4a) reveals that they are associated with water obducting predominantly in the Indian and Pacific oceans, respectively (Figures 4b and 4e; see Figure S9 for age histograms of all particles upwelling in the Indian and Pacific oceans). After first recirculating in the North Pacific subpolar gyre, the particles then predominantly follow either a relatively fast and direct pathway to the upwelling region in the western Indian Ocean via the Pacific western boundary current and the Indonesian Throughflow (Figures 4c and 4d; possibly related to high advection and mixing rates in this region) or a slow and indirect advective pathway to the eastern Pacific upwelling site via the western boundary currents, the tropical wind driven cells, and the circulation of the South Pacific subpolar gyre wherein the particles spend a long time before upwelling (Figures 4f and 4g).

It is noteworthy that the horizontal pathways of the PMOC water to its various global destinations do not differ much until after leaving the Northern Hemisphere (Figures 3c, 4c, and 4f). It is instead the vertical distribution of the particles that exerts greater control on the eventual route taken and the internal ocean processes acting at those depths. Indeed, separately mapping the origins of the particles that terminate in

the Indian, Pacific, and Southern oceans (Figure S10) shows that they originate from similar regions of the Pacific. The pathways do not appear to be strongly controlled by surface processes at the time of subduction.

4. Discussion and Conclusions

Using a fully coupled model simulation of the Pliocene ocean with an active PMOC, we have applied a Lagrangian ocean analysis to explicitly isolate the PMOC water at its North Pacific surface source locations and to subsequently determine its destinations, pathways, and timescales of inter-connectivity to the rest of the global oceans. Similar to the modern-day AMOC, we find that more than half of the PMOC water is upwelled in the Southern Ocean. However, one of our primary results is to verify a unique inter-connectivity of the Pliocene PMOC water masses with the tropical ocean, a feature that is weak for the AMOC water masses in our Pliocene and Control simulations (Figure S4) and in simulations of the present day (Figure S5; Döös & Coward, 1997). Of the 9.1 Sv of water subducting into the permanent thermocline of the northern North Pacific, approximately 15% obducts into the mixed layer of the tropical Indo-Pacific oceans. Of the remaining water, about 21% recirculates and returns to the surface of the North Pacific subpolar gyre, ∼57% advects toward the surface of the Southern Ocean, and the remainder in the Atlantic (∼2% in the tropics and ∼4.5% in subpolar latitudes). In comparison, of the 6.2 and 11.3 Sv of AMOC water in the Pliocene and Control runs, respectively, approximately 77% and 71%, respectively, upwell in the Southern Ocean. These are higher mainly due to their weak tropical connection.

Two distinct PMOC pathways to the tropical ocean exist, one primarily toward the Indian Ocean with a peak transit timescale of ∼250 years and another to the tropical South Pacific with a timescale of about ∼800 years (Figure 2). Transit timescales to the Southern Ocean are multi-centennial to millennial (Figures 2 and 3; Figures S4–S7). These advective pathways represent an important and, in the case of tropical PMOC inter-connectivity, unique feature of climates with an active PMOC and further research is required to understand the climatic and biogeochemical implications of such a link.

We emphasize that the distribution of transit times required for the subducted water to reach the tropical Indo-Pacific or the Southern Ocean is strongly skewed. While the maximum of the distribution may correspond to several centuries, the long tail of the distribution extends to several millennia.

The long multi-centennial to millennial timescales of connectivity raise the question of the role of diapycnal diffusion on the distribution of tracers on these timescales and how much the properties of water parcels following Lagrangian trajectories would change over those timescales. If we assume an average diapycnal diffusion coefficient of $\kappa_v = 3 \times 10^{-5}$ m^2 s^{-1}, consistent with typical zonal-mean values used in the Pacific in the model, and the average depth of the PMOC low branch $D = 2{,}000$ m, respectively, a scale analysis suggests a diffusion timescale $T = D^2/\kappa_v \approx 4{,}000$ years, which suggests that the PMOC and the water pathways connecting the North Pacific and the Southern Ocean below the mixed layer are approximately adiabatic, similar to the modern AMOC (e.g., Haertel & Fedorov, 2012). However, for water parcels traveling at intermediate depths before upwelling (e.g., Figure 4) and moving along the ocean boundaries, this diffusive timescale can easily become smaller by an order of magnitude and hence comparable to the parcels' transit time. For those parcels, diffusion can be important and can alter the tracers' concentration significantly before the parcels upwell into the mixed layer.

Some model dependence of the results is to be expected, particularly given the known sensitivity of particle trajectories to model resolution (Drake et al., 2018). Further, little is known about the possible PMOC strengths under different forcing conditions. Pathways and relative strengths could therefore be subject to many unknown variables; however, the model agreement to Pliocene observational proxies is impressive and gives confidence in the order one accuracy of the representation (Burls et al., 2017). Moreover, these results provide a blueprint of PMOC pathways regardless of the climate forcing used to achieve this state.

In this study, we present the first attempt to understand the water pathways and inter-connectivity in the presence of North Pacific deep water formation and an active PMOC cell as relevant to past climates in general. The different pathways of inter-connectivity found for the PMOC as compared to the modern AMOC, raise important questions about the varying role of ocean circulation during those climates.

Data Availability Statement

Data for the manuscript can be accessed at https://doi.org/10.5281/zenodo.4697546.

Acknowledgments
Partial funding support was provided to A. V. Fedorov by the Guggenheim Fellowship and by the ARCHANGE project (ANR-18-MPGA-0001, France). W. Liu is supported by the Alfred P. Sloan Foundation as a Research Fellow. N. J. Burls is supported by the National Science Foundation (NSF; OCN-1844380 and AGS-1756658), as well as the Alfred P. Sloan Foundation as a Research Fellow. The authors gratefully acknowledge Kaylea Nelson and Nicholas Grima for computing and technical support. Constructive comments from two anonymous reviewers that helped improve the manuscript were also greatly appreciated.

References

Arakawa, A., & Lamb, V. R. (1977). Computational design of the basic dynamical processes of the UCLA general circulation model. *Methods in Computational Physics*, *17*, 173–265. https://doi.org/10.1016/b978-0-12-460817-7.50009-4

Blanke, B., & Raynaud, S. (1997). Kinematics of the Pacific Equatorial Undercurrent: An Eulerian and Lagrangian approach from GCM results. *Journal of Physical Oceanography*, *27*(6):1038–1053. https://doi.org/10.1175/1520-0485(1997)027⟨1038:KOTPEU⟩2.0.CO;2

Burls, N. J., & Fedorov, A. V. (2014). Simulating Pliocene warmth and a permanent El Niño-like state: The role of cloud albedo. *Paleoceanography*, *29*(10), 893–910. https://doi.org/10.1002/2014pa002644

Burls, N. J., & Fedorov, A. V. (2017). Wetter subtropics in a warmer world: Contrasting past and future hydrological cycles. *Proceedings of the National Academy of Sciences of the United States of America*, *114*(49), 12888–12893. https://doi.org/10.1073/pnas.1703421114

Burls, N. J., Fedorov, A. V., Sigman, D. M., Jaccard, S. L., Tiedemann, R., & Haug, G. H. (2017). Active Pacific meridional overturning circulation (PMOC) during the warm Pliocene. *Science Advances*, *3*(9), e1700156. https://doi.org/10.1126/sciadv.1700156

Danabasoglu, G., Bates, S. C., Briegleb, B. P., Jayne, S. R., Jochum, M., Large, W. G., et al. (2012). The CCSM4 ocean component. *Journal of Climate*, *25*(5), 1361–1389. https://doi.org/10.1175/JCLI-D-11-00091.1

Döös, K., & Coward, A (1997). The Southern Ocean as the major upwelling zone of North Atlantic deep water. *International WOCE Newsletter*, *27*, 3–4.

Drake, H. F., Morrison, A. K., Griffies, S. M., Sarmiento, J. L., Weijer, W., & Gray, A. R. (2018). Lagrangian timescales of Southern Ocean upwelling in a hierarchy of model resolutions. *Geophysical Research Letters*, *45*(2), 891–898. https://doi.org/10.1002/2017gl076045

Emile-Geay, J., Cane, M. A., Naik, N., Seager, R., Clement, A. C., & van Geen, A. (2003). Warren revisited: Atmospheric freshwater fluxes and "why is no deep water formed in the North Pacific". *Journal of Geophysical Research*, *108*(C6). https://doi.org/10.1029/2001jc001058

Fedorov, A. V., Burls, N. J., Lawrence, K. T., & Peterson, L. C. (2015). Tightly linked zonal and meridional sea surface temperature gradients over the past five million years. *Nature Geoscience*, *8*(12), 975–980. https://doi.org/10.1038/ngeo2577

Ferreira, D., Cessi, P., Coxall, H. K., De Boer, A., Dijkstra, H. A., Drijfhout, S. S., et al. (2018). Atlantic-Pacific asymmetry in deep water formation. *Annual Review of Earth and Planetary Sciences*, *46*, 327–352. https://doi.org/10.1146/annurev-earth-082517-01004510.1146/annurev-earth-082517-010045

Ferreira, D., Marshall, J., & Campin, J.-M. (2010). Localization of deep water formation: Role of atmospheric moisture transport and geometrical constraints on ocean circulation. *Journal of Climate*, *23*(6), 1456–1476. https://doi.org/10.1175/2009jcli3197.1

Gent, P. R., & McWilliams, J. C. (1990). Isopycnal Mixing In Ocean Circulation Models. *Journal of Physical Oceanography*, *20*(1), 150–155. https://doi.org/10.1175/1520-0485(1990)020⟨0150:IMIOCM⟩2.0.CO;2

Haertel, P., & Fedorov, A. (2012). The ventilated ocean. *Journal of Physical Oceanography*, *42*(1):141–164. https://doi.org/10.1175/2011JPO4590.1

Johnson, H. L., Cessi, P., Marshall, D. P., Schloesser, F., & Spall, M. A. (2019). Recent contributions of theory to our understanding of the Atlantic meridional overturning circulation. *Journal of Geophysical Research: Oceans*, *124*(8), 5376–5399. https://doi.org/10.1029/2019jc015330

Jones, C. S., & Cessi, P. (2016). Interbasin transport of the meridional overturning circulation. *Journal of Physical Oceanography*, *46*(4), 1157–1169. https://doi.org/10.1175/jpo-d-15-0197.1

Jones, C. S., & Cessi, P. (2017). Size matters: Another reason why the Atlantic is saltier than the Pacific. *Journal of Physical Oceanography*, *47*(11), 2843–2859. https://doi.org/10.1175/jpo-d-17-0075.1

Kuhlbrodt, T., Griesel, A., Montoya, M., Levermann, A., Hofmann, M., & Rahmstorf, S. (2007). On the driving processes of the Atlantic meridional overturning circulation. *Reviews of Geophysics*, *45*(1). https://doi.org/10.1029/2004rg000166

Large, W. G., McWilliams, J. C., & Doney, S. C. (1994). Oceanic vertical mixing: A review and a model with a nonlocal boundary layer parameterization. *Reviews of Geophysics*, *32*(4), 363–403. https://doi.org/10.1029/94rg01872

LaRiviere, J. P., Ravelo, A. C., Crimmins, A., Dekens, P. S., Ford, H. L., Lyle, M., & Wara, M. W. (2012). Late Miocene decoupling of oceanic warmth and atmospheric carbon dioxide forcing. *Nature*, *486*(7401), 97–100. https://doi.org/10.1038/nature11200

Lear, C. H., Elderfield, H., & Wilson, P. A. (2000). Cenozoic deep-sea temperatures and global ice volumes from mg/ca in benthic foraminiferal calcite. *Science*, *287*(5451), 269–272. https://doi.org/10.1126/science.287.5451.269

Liu, W., & Hu, A. (2015). The role of the PMOC in modulating the deglacial shift of the ITCZ. *Climate Dynamics*, *45*(11–12), 3019–3034. https://doi.org/10.1007/s00382-015-2520-6

McCreary, J. P., & Lu, P. (1994). Interaction between the Subtropical and Equatorial Ocean circulations – the Subtropical Cell. *Journal of Physical Oceanography*, *24*(2):466–497.

Ortega, P., Robson, J., Sutton, R. T., & Andrews, M. B. (2017). Mechanisms of decadal variability in the Labrador Sea and the wider North Atlantic in a high-resolution climate model. *Climate Dynamics*, *49*(7), 2625–2647. https://doi.org/10.1007/s00382-016-3467-y

Pagani, M., Liu, Z., LaRiviere, J., & Ravelo, A. C. (2010). High Earth-system climate sensitivity determined from Pliocene carbon dioxide concentrations. *Nature Geoscience*, *3*(1), 27–30. https://doi.org/10.1038/ngeo724

Saenko, O. A., Schmittner, A., & Weaver, A. J. (2004). The Atlantic-Pacific seesaw. *Journal of Climate*, *17*(11), 2033–2038. https://doi.org/10.1175/1520-0442(2004)017<2033:tas>2.0.co;2

Schmittner, A., Silva, T. A. M., Fraedrich, K., Kirk, E., & Lunkeit, F. (2011). Effects of mountains and ice sheets on global ocean circulation*. *Journal of Climate*, *24*(11), 2814–2829. https://doi.org/10.1175/2010jcli3982.1

Spall, M. A. (1992). Cooling spirals and recirculation in the subtropical gyre. *Journal of Physical Oceanography*, *22*(5), 564–571. https://doi.org/10.1175/1520-0485(1992)022<0564:csarit>2.0.co;2

Spall, M. A., & Pickart, R. S. (2001). Where does dense water sink? A subpolar gyre example*. *Journal of Physical Oceanography*, *31*, 810–826. https://doi.org/10.1175/1520-0485(2001)031<0810:wddwsa>2.0.co;2

Stocker, T. F., & Wright, D. G. (1991). Rapid transitions of the ocean's deep circulation induced by changes in surface water fluxes. *Nature*, *351*(6329), 729–732. https://doi.org/10.1038/351729a0

Thomas, M. D., & Fedorov, A. V. (2017). The eastern subtropical pacific origin of the equatorial cold bias in climate models: A Lagrangian perspective. *Journal of Climate*, *30*(15):5885–5900. https://doi.org/10.1175/JCLI-D-16-0819.1

Thomas, M. D., Tréguier, A.-M., Blanke, B., Deshayes, J., & Voldoire, A. (2015). A Lagrangian method to isolate the impacts of mixed layer subduction on the meridional overturning circulation in a numerical model. *Journal of Climate*, *28*(19):7503–7517. https://doi.org/10.1175/JCLI-D-14-00631.1

Toggweiler, J. R., & Samuels, B. (1995). Effect of drake passage on the global thermohaline circulation. *Deep Sea Research Part I: Oceanographic Research Papers*, *42*(4), 477–500. https://doi.org/10.1016/0967-0637(95)00012-u

van Sebille, E., Griffies, S. M. R. A., Abernathey, R., Adams, T. P., Berloff, P., Biastoch, A., et al. (2018). Lagrangian ocean analysis: Fundamentals and practices. *Ocean Modelling*, *121*, 49–75. https://doi.org/10.1016/j.ocemod.2017.11.008

van Sebille, E., Spence, P., Mazloff, M. R., England, M. H., Rintoul, S. R., & Saenko, O. A. (2013). Abyssal connections of Antarctic bottom water in a Southern Ocean state estimate. *Geophysical Research Letters*, *40*(10), 2177–2182. https://doi.org/10.1002/grl.50483

Warren, B. A. (1983). Why is no deep water formed in the North Pacific? *Journal of Marine Research*, *41*(2), 327–347. https://doi.org/10.1357/002224083788520207

Woodard, S. C., Rosenthal, Y., Miller, K. G., Wright, J. D., Chiu, B. K., & Lawrence, K. T. (2014). Antarctic role in northern hemisphere glaciation. *Science*, *346*(6211), 847–851. https://doi.org/10.1126/science.1255586

Xie, L., & Hsieh, W. W. (1995). The global distribution of wind-induced upwelling. *Fisheries Oceanography*, *4*(1), 52–67. https://doi.org/10.1111/j.1365-2419.1995.tb00060.x

Erratum

In the originally published version of this article, two citations of a reference were incorrectly noted as Döös & Webb, 1997 in the main text instead of Döös & Coward, 1997. These citations have been corrected, and the present version may be considered the authoritative version of record.